THE JOURNAL OF BIOLOGICAL CHEMISTRY VOL. 287, NO. 35, pp. 29417–29428, August 24, 2012

NMR Structure of *Carcinoscorpius rotundicauda* Thioredoxin-related Protein 16 and Its Role in Regulating Transcription Factor NF-κB Activity*

Received for publication, May 22, 2012, and in revised form, June 19, 2012 Published, JBC Papers in Press, July 3, 2012, DOI 10.1074/jbc.M112.379859

Pankaj Kumar Giri[‡1], **Fan Jing-Song**[‡], **Muthu K. Shanmugam**[§], **Jeak Ling Ding**[‡], **Gautam Sethi**[§], **Kunchithapadam Swaminathan**[‡2], **and J. Sivaraman**[‡3]

From the Departments of [‡]*Biological Sciences and* [§]*Pharmacology, National University of Singapore, Singapore 117543*

Background: Cr-TRP16 is a thioredoxin like protein that regulates NF-κB activity.
Results: NMR structure of Cr-TRP16, along with its regulation of NF-κB activity, is reported.
Conclusion: Our findings elucidate molecular mechanism by which NF-κB activation is regulated through Cr-TRP16.
Significance: This study helps further in understanding the interactions of Trxs and Trx-like proteins with other metabolic pathways and will lead to promising therapeutic development.

Thioredoxins (Trxs), which play a key role in maintaining a redox environment in the cell, are found in almost all organisms. Trxs act as potential reducing agents of disulfide bonds and contain two vicinal cysteines in a C*XX*C motif at the active site. Trx is also known to activate the DNA binding activity of NF-κB, an important transcription factor. Previously, Trx-related protein 16 from *Carcinoscorpius rotundicauda* (Cr-TRP16), a 16-kDa Trx-like protein that contains a WCPPC motif, was reported. Here we present the NMR structure of the reduced form of Cr-TRP16, along with its regulation of NF-κB activity. Unlike other 16-kDa Trx-like proteins, Cr-TRP16 contains an additional Cys residue (Cys-15, at the N terminus), through which it forms a homodimer. Moreover, we have explored the molecular basis of Cr-TRP16-mediated activation of NF-κB and showed that Cr-TRP16 exists as a dimer under physiological conditions, and only the dimeric form binds to NF-κB and enhances its DNA binding activity by directly reducing the cysteines in the DNA-binding motif of NF-κB. The C15S mutant of Cr-TRP16 was unable to dimerize and hence does not bind to NF-κB. Based on our finding and combined with the literature, we propose a model of how Cr-TRP16 is likely to bind to NF-κB. These findings elucidate the molecular mechanism by which NF-κB activation is regulated through Cr-TRP16.

Reactive oxygen species are natural by-products of several oxidative metabolic pathways and are known to mediate intracellular signaling pathways (1). However, excessive production of reactive oxygen species is detrimental to the cell, because of increased oxidative stress (2). Thioredoxin (Trx)[4] plays a key role in maintaining an intracellular redox state, which is essential for protecting cells from oxidative damage (3). Trx is a 12-kDa ubiquitous and evolutionarily conserved protein in almost all organisms and functions as a disulfide reductase (4, 5). A conserved Cys-Xaa-Xaa-Cys sequence at the active site of Trx is involved in either reducing disulfide bonds or oxidizing sulfhydryls, both intra- and extracellularly (6). The two cysteines are maintained in an active reduced form by Trx reductase, a selenocysteine-containing protein that uses the reducing power of NADPH (6). The disulfide reductase activity and reduction potential of the cysteines depend largely on the identity of the two *XX* residues (7).

Trx proteins also function as a redox sensor and transducer that impart information on the cellular redox status to proteins that do not possess their own redox-sensitive residues. For instance, the reduced form of Trx1, a mammalian cytosolic isoform, binds to and thereby inhibits the activity of apoptosis signal-regulating kinase 1 (ASK1), an upstream activator of the JNK and p38 MAPK signaling pathways (8). Their alterations have been implicated in cardiovascular diseases (9), diabetes (10), hepatic and renal diseases (11), Alzheimer disease (12), Parkinson disease (13), and rheumatoid arthritis (14). Some human cancers show greatly increased Trx expression (15, 16), indicating a potential role for Trx in tumorigenesis. Its interactions with different proteins of the metabolic and signaling pathways make Trx an attractive target for therapeutic interventions.

There are several Trx-like proteins, which possess the thioredoxin fold and function and exist in different sizes (12–32 kDa). Recently, a 16-kDa protein that contains a WCPPC motif has been isolated and characterized from a species of horseshoe crab, *Carcinoscorpius rotundicauda*, and named Trx-related protein 16 (Cr-TRP16) (17). Notably, the 16-kDa Trx-like pro-

* This work was supported in part by a grant from the Biomedical Research Council, Singapore, Grants R154000461305 (to J. S.) and R154-000-424-305 (to K. S.). This project was also supported in part by a grant from Singapore Ministry of Health National Medical Research Council (to. G. S.) under its Individual Research Grant (IRG) funding scheme.

The atomic coordinates and structure factors (code 2LUS) have been deposited in the Protein Data Bank, Research Collaboratory for Structural Bioinformatics, Rutgers University, New Brunswick, NJ (http://www.rcsb.org/).

[1] Supported by a graduate research scholarship from the National University of Singapore.

[2] To whom correspondence may be addressed. Tel.: 65-6516-7932; Fax: 65-6779-2486; E-mail: dbsks@nus.edu.sg.

[3] To whom correspondence may be addressed. Tel.: 65-6516-1163; Fax: 65-6779-2486; E-mail: dbsjayar@nus.edu.sg.

[4] The abbreviations used are: Trx, thioredoxin; HSQC, heteronuclear single quantum coherence; RMSD, root mean square deviation; AUC, analytical ultracentrifugation.

teins are functionally similar to the 12-kDa Trxs, and each monomer contains two Cys residues at the active site. Unlike other 16-kDa Trx like proteins, Cr-TRP16 contains an additional Cys residue (Cys-15, at the N terminus), but it lacks the extra C-terminal Cys residue, which is found in mammalian Trxs (18).

A subtle balance between oxidants and antioxidants is crucial for homeostasis. There is emerging evidence that the highly conserved intracellular redox state regulates the mechanism of signal transduction and gene expression (19). NF-κB is one of the redox-regulated proteins. It is a member of the Rel family of transcription factors and exists in the cytoplasm in complex with its inhibitor protein, IκB (20). A wide variety of stimuli, including TNF-α, phorbol ester, bacterial lipopolysaccharide, and virus infection, can activate NF-κB (21). NF-κB activation involves site-specific phosphorylation of IκB-α, which results in the dissociation of the complex, unmasking of the NF-κB nuclear localization signal, and nuclear entry of NF-κB to bind to its cognate DNA (22). Thus, for the stimuli that potently and rapidly modulate the nuclear activity of NF-κB, the IκB-α may represent a critical activation target (20). Several studies have suggested that Trx is a specifically potent antioxidant for NF-κB activation (23). Similar to the human Trx1, Cr-TRP16 also up-regulates the TNFα-induced NF-κB activation.

Cr-TRP16 exists as a dimer in the oxidized state. However, the underlying mechanism of dimerization and the regulation of NF-κB by Cr-TRP16 are so far unknown. For example, what is the physiological role of the Trx-dimer? Is Cys-15 involved in Cr-TRP16 dimer formation? How is NF-κB regulated under oxidized and reduced cellular environments? It is possible that the oxidation-induced dimerization facilitates sensing cellular oxidative stress. Dimerization might remove the Trx from the redox cycle, which is catalyzed by Trx reductase because the dimer is not a suitable substrate for Trx reductase. In addition, dimerization of secreted Trx in the relatively oxidizing extracellular environment could be a way of limiting the growth-stimulating effects of Trx (24). Further mutational and structural studies will define the function of the additional N-terminal Cys-15 residue in Cr-TRP16. To understand the NF-κB regulation by Cr-TRP16 and to address the above questions, we had undertaken the structural and functional characterization of Cr-TRP16, the first Trx fold structure from an ancient arthropod. Here we report the NMR structure of the reduced form of wild type Cr-TRP16. Moreover, the role of the Cys-15 residue in dimerization and NF-κB regulation were studied by site-directed mutagenesis, biophysical, and immunoprecipitation techniques.

EXPERIMENTAL PROCEDURES

Cloning—The full-length Cr-TRP16 gene (encoding residues Met-1–Arg-143) was PCR-amplified using a forward (CAGCATATGATGGAATTTATCCAAGGAAT) and a reverse (CCTCTCGAGTCTTGCCCAGTT) primer with an NdeI restriction site at the 5′ end and an XhoI site at the 3′ end (underlined), respectively, and inserted into the pET-22b(+) vector (Invitrogen), which was previously linearized by the corresponding restriction enzymes. For mammalian expression, the Cr-TRP16 gene was PCR-amplified with the following primers: forward, GGAGGATCCATGGAATTTATCCAAGGA, and reverse, ATTCTCGAGTCATTTGTCGTCATCGTCCTTATAGTCTCTTGCCCAGTTCTGGAA, which contained BamHI and XhoI restriction sites (underlined), respectively. The reverse primer introduced a FLAG tag at the C terminus of the Cr-TRP16 protein. The insert was ligated into the previously linearized expression vector pcDNA3.1/V5-His/lacZ (Invitrogen).

Protein Expression and Purification—The pET22b:Cr-TRP16 construct was transformed into the bacterial strain *Escherichia coli* BL21(DE3) for expression. Optimal expression of the Cr-TRP16 protein was achieved by induction of 1-liter culture with 0.3 mM isopropyl β-D-1-thiogalactopyranoside at 20 °C. The cells were disrupted by a French press, and the supernatant was collected after centrifuging at 10,000 × *g* for 1 h at 4 °C. His-tagged Cr-TRP16 proteins were purified in two steps using nickel-nitrilotriacetic acid (Qiagen) affinity chromatography followed by a Superdex 75 gel filtration column on Äkta Express (GE Healthcare). The buffer was exchanged to a solution containing 10 mM Tris (pH 7.0), 100 mM NaCl, 5 mM dithiothreitol, 5% glycerol, 1 mM EDTA, and finally the protein was concentrated to 18 mg/ml. For NMR study, ^{15}N-labeled and ^{13}C,^{15}N-double labeled samples were prepared using M9 minimal medium with $^{15}NH_4Cl$ and [^{13}C]glucose as a sole source of nitrogen and carbon, respectively. Weakly aligned ^{15}N-labeled sample was prepared by the addition of 8 mg ml^{-1} of filamentous phage Pf1 (from ASLA Biotech) for residue dipolar coupling measurement.

NMR Experiments and Structure Determination—All NMR experiments were carried out at 25 °C on a Bruker Avance 800 MHz spectrometer equipped with a TXI cryogenic probe. ^{1}H, ^{13}C, and ^{15}N resonance assignments were performed by measuring the three-dimensional HNCACB, three-dimensional CBCA(CO)NH (25), and three-dimensional CCH-TOCSY (26) spectra. Interproton distance restraints for structural calculation were obtained from three-dimensional ^{13}C-edited NOESY-HSQC, three-dimensional ^{15}N-edited NOESY-HSQC, and two-dimensional NOESY spectra using a 100-ms mixing time. $^{1}D_{NH}$ residue dipolar couplings were measured using the IPAP method (27). The residue dipolar coupling values were obtained by subtracting the reference value in isotropic solution. Two- and three-dimensional NMR spectra were processed using the NMRPipe program (28), and data analysis was performed with the help of the Sparky program (29).

The structure was calculated using the Xplor-NIH 2.24 software package (30). A total of 1731 NOE distance restraints, 76 hydrogen bonds, and 124 dihedral angle restraints were predicted by the TALOS program (31). Residue dipolar couplings were used in the final cooling stage. 100 structures were calculated using 30,000 steps of simulated annealing, and a final ensemble of 20 lowest energy structures was selected for figure preparation.

Site-directed Mutagenesis—On the NMR structure of Cr-TRP16, Cys-15 is located on the surface and has been hypothesized to be involved in dimerization. This residue was mutated to serine in both the pET22b and pcDNA3.1/V5-His/lacZ constructs by the use of the inverse PCR-based mutagenesis protocol (32). The C15S mutant protein was

expressed following the steps that were described for the wild type protein.

Analytical Ultracentrifugation (AUC)—The dimeric state of WT and C15S mutant Cr-TRP16 proteins purified by affinity and gel filtration followed by reverse phase HPLC (data not shown) was investigated by monitoring their sedimentation properties in sedimentation velocity experiments. 500 μl of samples at $A_{280\ nm}$ of 0.8 in 10 mM Tris-HCl (pH 7.0), 100 mM NaCl, and 5% glycerol were used. The experiments were carried out in the absence of DTT in the buffer. Sedimentation velocity profiles were collected by monitoring the absorbance at 280 nm. The samples were centrifuged at 40,000 rpm at 20 °C in a Beckman Optima XL-I centrifuge fitted with a six-hole AN-60 rotor and double-sector aluminum centerpieces and equipped with absorbance optics. The scans were analyzed using the Sedfit program (33).

Western Blotting—The human cervical epithelial carcinoma (HeLa) cell line was obtained from American Type Culture Collection (Manassas, VA). It has to be noted that no horseshoe crab cell line is available, and HeLa are the most commonly used cells for thioredoxin related (including Cr-TRP16) *ex vivo* studies (17, 23, 34, 35). The cells were cultured in RPMI 1640 medium containing 1× antibiotic-antimycotic solution with 10% FBS. HeLa cells transfected with the Cr-TRP16 or C15S Cr-TRP16 plasmids were lysed in lysis buffer (20 mM Tris (pH 7.4), 250 mM NaCl, 2 mM EDTA (pH 8.0), 0.1% Triton X-100, 0.01 mg/ml aprotinin, 0.005 mg/ml leupeptin, 1 mM PMSF, and 4 mM $NaVO_4$). The lysates were then spun on a microcentrifuge at 14,000 rpm for 10 min to remove insoluble material and resolved on 10% SDS gel. Nuclear protein extracts were prepared using a nuclear extraction kit (Active Motif, Carlsbad, CA) according to the manufacturer's instructions. Protein concentration was determined with the Bradford reagent, and 30 μg of nuclear or cytoplasmic extract was taken for immunoblotting. After electrophoresis, the proteins were electrotransferred to a nitrocellulose membrane, blocked with 5% nonfat milk, and probed overnight with the antibodies of interest at 4 °C. The blot was washed, exposed to HRP-conjugated secondary antibodies for 1 h, and finally examined by ECL (Amersham Biosciences).

NF-κB DNA Binding Assay—To determine NF-κB activation, we performed DNA binding assay using the TransAM NF-κB kit (Active Motif) according to the manufacturer's instructions and as previously described (36). Briefly, HeLa cells were transfected with the Cr-TRP16 or C15S Cr-TRP16 plasmids for 30 h and then stimulated with TNF-α (1 nM) for 6 h. Nuclear protein extracts were prepared using a nuclear extraction kit (Active Motif) according to the manufacturer's instructions. Protein concentration was determined with the Bradford reagent, and 20 μg of nuclear extract was added to the plates precoated with an NF-κB consensus oligonucleotide sequence and incubated at room temperature for 1 h with continuous shaking at 100 rpm. The plates were washed and incubated with a p65 primary antibody for 1 h at room temperature. After the final incubation with a secondary antibody, the wells were washed with washing buffer; color was developed by the addition of substrate solution and read after 10 min at 450 nm against a blank, which was read at a reference wavelength of 655 nm.

NF-κB-dependent Luciferase Reporter Assay—NF-κB dependent reporter gene expression assay was performed as described previously (37). Briefly, ~10^5/well HeLa cells were plated in 96-well plates in RPMI buffer containing 10% FBS. The NF-κB-responsive elements, linked to a luciferase reporter gene plasmid, were transfected with the wild type Cr-TRP16 or C15S Cr-TRP16 (mutant) plasmids. Transfection was performed using Lipofectamine (Invitrogen) according to the manufacturer's protocols. After 30 h of transfection, HeLa cells were treated with TNF-α (1 nM) for 6 h and then washed and lysed in luciferase lysis buffer (Promega). Luciferase activity was measured by Tecan (Durham, NC) plate reader, which is equipped with a function to measure luminescence by using a luciferase assay kit (Promega) and was normalized to β-galactosidase activity. All of the luciferase experiments were performed in triplicate and repeated three or more times.

DNA Binding Assay of NF-κB/p65 C38S Mutant—To further explore the mechanism of interaction between Cr-TRP16 and NF-κB, we undertook an *ex vivo* study to demonstrate that Cr-TRP16 exists as a dimer inside cell and directly reduces the Cys-38 of NF-κB p65 subunit. We used expression plasmids that encode p65 wild type and C38S mutated p65. The advantage of using transfected cells overexpressing p65 is that there is no TNF-α stimulation needed to observe the direct effect of Cr-TRP16 on NF-κB DNA binding activity. Briefly, HeLa cells were transfected with the plasmids pcDNA3.1, pcDNA-p65, and pcDNA-p65C38S (a gift from Dr. Gilmore, Boston University), along with Cr-TRP16 or C15S Cr-TRP16 for 36 h.

Nuclear protein extracts were prepared using a nuclear extraction kit (Active Motif) according to the manufacturer's instructions. Protein concentration was determined with the Bradford reagent, and 20 μg of nuclear extract was added to the plates that were precoated with NF-κB consensus sequence oligonucleotide and incubated at room temperature for 1 h with continuous shaking at 100 rpm. The plates were washed and incubated with p65 primary antibody for 1 h at room temperature. After the final incubation with secondary antibody, the wells were washed with washing buffer, and color was developed by the addition of substrate solution, which was read at 450 nM against the blank, reference wavelength of 655 nM after 10–15 min. Western blot analysis was performed to determine the expression levels of p65 and p65C38S. The experiments were repeated three times with almost identical outcome.

RESULTS

Overall Structure—The structure of full-length Cr-TRP16 (143 amino acids) was solved by NMR and refined to a final RMSD of 0.51 ± 0.11 Å (backbone) (Table 1) for the 20 best structures (Fig. 1*A*). Cr-TRP16 consists of seven β-strands in two β-sheets (Fig. 1, *B* and *C*), similar to other Trxs. The first β-sheet accommodates both parallel and anti-parallel strands (β7 ↑ β6 ↓ β3 ↑ β4 ↑ β5 ↑). The residues of strands β3 and β4 are mostly buried and conserved in thioredoxins. These residues are mostly hydrophobic and are part of a hydrophobic cluster, formed by Phe-31, Tyr-32, Phe-33, Phe-35, Trp-37, Phe-44, Tyr-52, Phe-62, Phe-66, Phe-77 Tyr-79, Trp-87, Tyr-

TABLE 1
NMR data and structure determination details for reduced Cr-TRP16

Parameters	
All NOE distance restraints[a]	1728
Intraresidue	717
Inter-residue	
Sequential ($\|i - j\| = 1$)	435
Medium range ($1 < \|i - j\| \leq 5$)	227
Long range ($\|i - j\| \geq 5$)	349
Hydrogen bond restraints	76
Dihedral angle restraints (φ, ψ)[b]	124
Residual dipolar coupling restraints	54
Deviations from idealized covalent geometry[c]	
RMSD of bond lengths (Å)	0.0021 ± 0.00004
RMSD of bond angles (°)	0.3634 ± 0.0086
RMSD of improper angles (°)	0.3329 ± 0.008
Deviations from experimental restraints	
RMSD of distance restraints (Å)	0.0231 ± 0.0005
RMSD of dihedral angle restraints (°)	0.2170 ± 0.057
Ramachandran plot analysis (%)[d]	
Residues in allowed regions	95.5%
Residues in generously allowed regions	3.0%
Residues in disallowed regions	1.5%
Average RMSD from mean structure (Å)[e]	
All residues (2–141)	0.72 ± 0.15
Regular 2° structure region	0.47 ± 0.10

[a] The distance restraints were obtained by classifying the NOE cross-peaks into three categories: strong (1.8–2.9 Å), medium (1.8–3.5 Å), and weak (1.8–5.0 Å).
[b] Dihedral angles of backbone φ and ψ were predicted by TALOS (31) using the chemical shifts of Cα, Cβ, Hα, N, and HN.
[c] The twenty lowest energy conformers with no NOE violations greater than 0.3 Å and no torsion angle violations greater than 3° were selected from 100 conformers to represent the NMR ensembles.
[d] Calculated with PROCHECK NMR (63).
[e] Calculated with MOLMOL (64). The averages are over backbone atoms. The 2° structure regions are: 8–11, 15–18, 28–33, 45–57, 62–66, 73–82, 88–90, 95–104, 111–116, 127–133, and 137–141.

92, and Tyr-104. The second β-sheet, formed as a β-hairpin (β1 ↑ β2 ↓), is solvent-accessible and carries five charged residues: Lys-11, Lys-12, Arg-14, Glu-16, and Glu-21. This segment is highly variable among thioredoxin-like proteins. The longest helix, α1 (residues 43–57), is located on the surface of the protein.

Sequence and Structural Homology—Proteins with the Trx fold and active site sequence are classified under the Trx superfamily (38). Comparison of Trxs and Trx like protein sequences (Fig. 2*A*) show that the Trx core domain is well conserved with the central five β-strands, surrounded by four α-helices (39). Cr-TRP16 has an overall sequence identity of 18% with the 12-kDa Trxs from mammalian, insect, and bacterial species. Most invariant residues are clustered around the active site. The 12-kDa Trxs are characterized by a conserved WCGPC motif in the active site, whereas Cr-TRP16 has a WCPPC motif.

So far, no Trx structure is reported from the subphylum (Celicerata) to which horseshoe crab belongs (noninsect species of arthropods). A search for topologically similar domains in the Protein Data Bank using the DALI program (40) reveals that the structural features of Cr-TRP16 resemble a typical Trx (41). The closest match is observed between the Trx-related protein *tryparedoxin II* (Protein Data Bank code 1FG4), a 16-kDa Trx-like protein from *Crithidia fasciculate* with 26% sequence identity, and an RMSD of 2.9 Å for 126 Cα atoms. The structure-based sequence alignment reveals that most of the structurally invariant residues are located at the N-terminal loop region between β2 and β3 (Fig. 2).

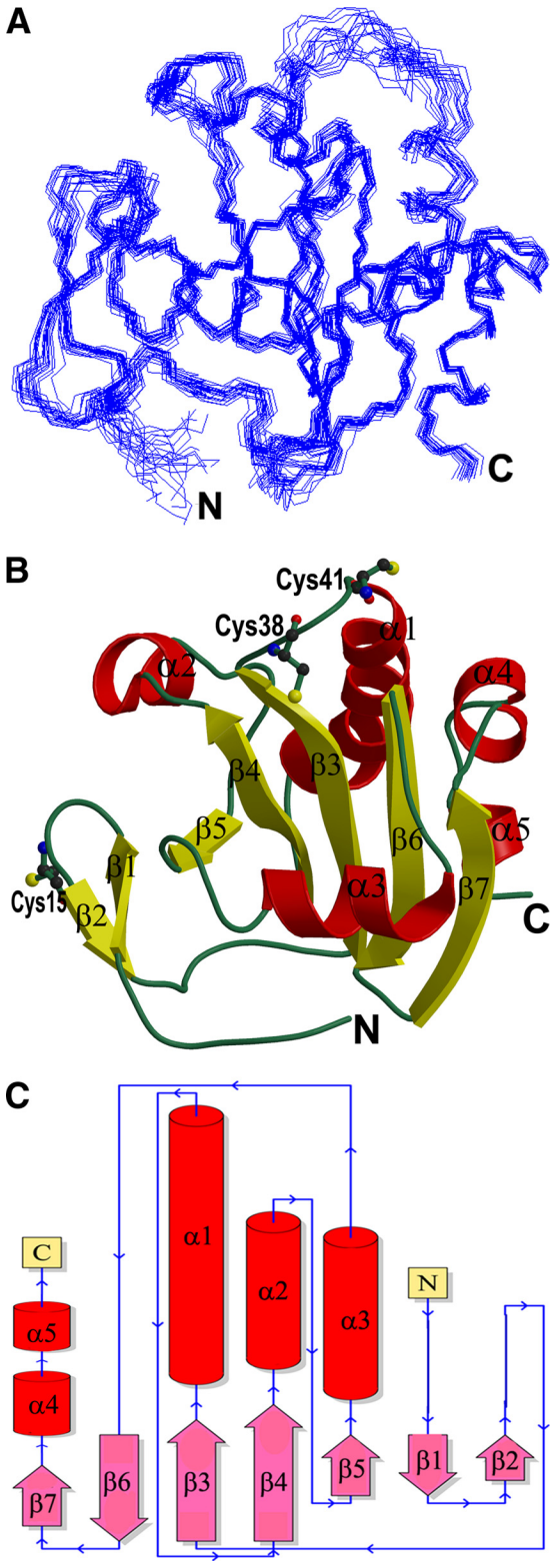

FIGURE 1. **Structure of Cr-TRP16.** *A*, the best 20 backbone structures of reduced WT Cr-TRP16 thioredoxin after simulated annealing refinement. *B*, the ribbon diagram of the Cr-TRP16 molecule. Cr-TRP16 consists of seven β-strands in two β-sheets, similar to other Trxs. The first β-sheet (β1β2) is an anti-parallel β-hairpin, and the second β-sheet contains both parallel and anti-parallel strands (β7 ↑ β6 ↓ β3 ↑ β4 ↑ β5 ↑). There are four α-helices (α1, α2, α3, and α4). The active site cysteines (Cys-38 and Cys-41) and the N-terminal Cys-15 residue that promotes dimerization are drawn as ball-and-sticks. This figure and Fig. 2*A* were prepared using the program Molscript (59). *C*, the topology diagram of Cr-TRP16.

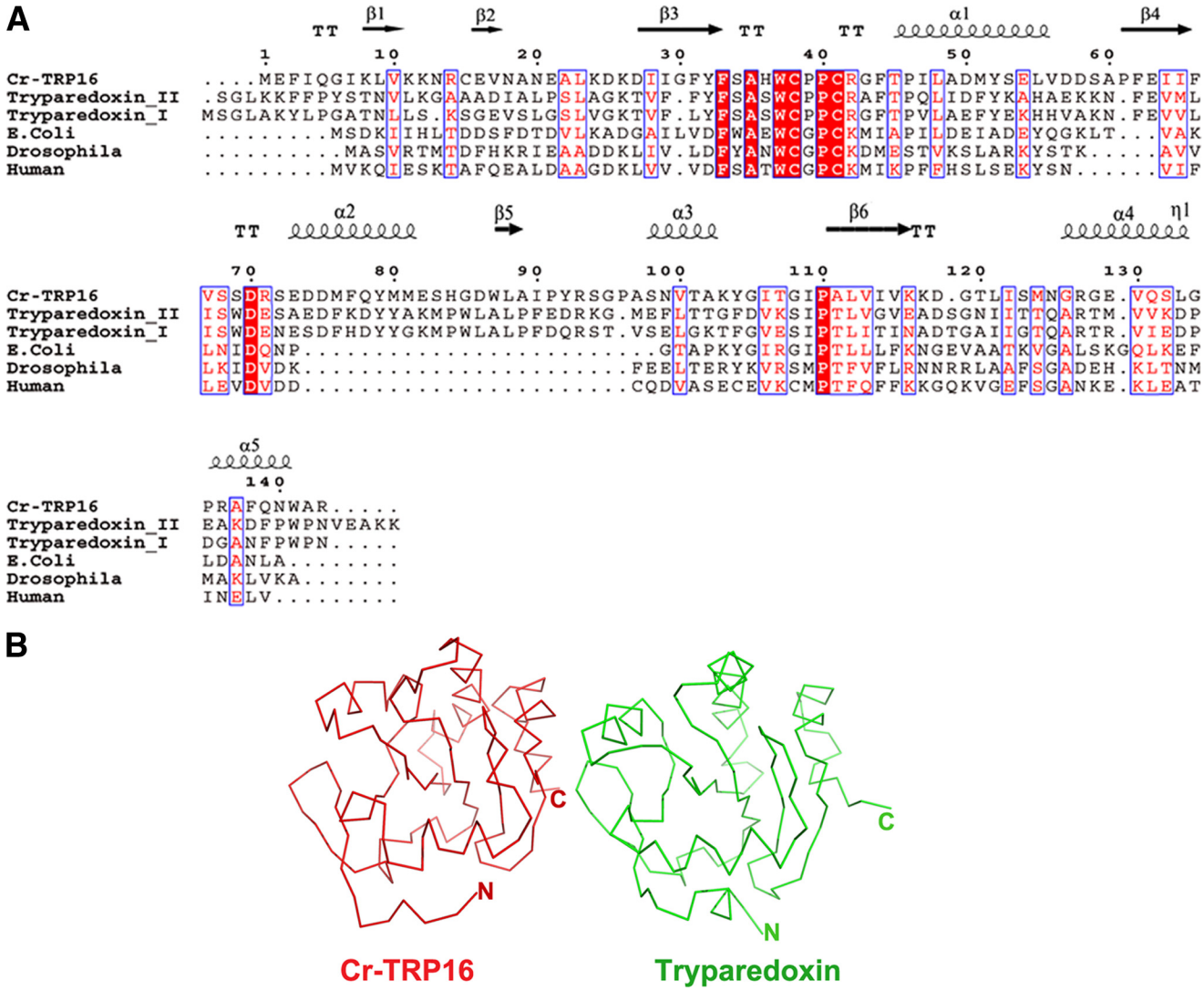

FIGURE 2. **Comparison of Cr-TRP16 with Trypaerdoxin.** *A*, structure-based sequence comparison between Cr-TRP16 and other 16- and 12-kDa thioredoxins. Alignment was done by Clustal W. Identical and conserved residues are highlighted in *red* and outlined in *blue*, respectively. This figure was created by using the program ESPript (60). *B*, comparison of Cr-TRP16 (*red*) and Trypaerdoxin II (*green*) (Protein Data Bank code 1FG4) from *C. fasciculate*. The alignment was performed using the program COOT (61). The RMSD between is 2.9 Å for 126 Cα atoms.

Dimerization of Cr-TRP16—Human 12-kDa Trx1 forms a homodimer through an intermolecular disulfide bond via Cys-73 (18). Interestingly, Cr-TRP16 can also form a stable dimer. Despite low sequence identity (18%) between Cr-TRP16 and hTrx1, Cr-TRP16 could also enhance TNFα-induced NF-κB transcriptional activation by increasing the NF-κB DNA binding activity. In addition to the two conserved Cys residues (Cys-38 and Cys-41) at the active site, Cr-TRP16 has an additional Cys residue at position 15, which is involved in the formation of an intermolecular disulfide bond. The previous mass spectrometry report (17) has shown that only the two conserved Cys residues at the active site are redox active, similar to the human Trx1. To further explore the role of Cys-15 in dimer formation, we have performed two-dimensional HSQC experiments for oxidized and reduced wild type Cr-TRP16 and analytical ultracentrifuge experiments on oxidized and reduced wild type and C15S mutant Cr-TRP16.

^{1}H-^{15}N-HSQC NMR Spectroscopy—To characterize the mode of dimerization and to identify the critical residues involved in dimer formation, the ^{1}H-^{15}N-HSQC NMR spectra of reduced and oxidized wild type Cr-TRP16 were compared. Sequential assignments were completed by using the standard triple-resonance methods. The assigned spectra of reduced and the overlay ^{1}H-^{15}N-HSQC NMR spectra of reduced and oxidized Cr-TRP16 are shown in Fig. 3, respectively. Two-dimensional NMR experiments show that the majority of the amides are unaffected by dimerization. Fig. 3*B* shows that a total of 26 amide signal chemical shifts have changed. Nearly all of these residues are located in the surface-exposed region around the N terminus Cys-15 and the second β-sheet (β1β2). This suggests that this part of the molecule is involved in dimerization.

Analytical Ultracentrifugation—The C15S (C15S) mutant was generated to elucidate the role of the additional Cys at position 15 (Cys-15) in dimer formation and its physiological significance in the NF-κB function. Dynamic light scattering measurements on reduced and oxidized C15S Cr-TRP16 show an apparent molecular mass corresponding to only a monomer. Nonreducing and SDS-PAGE for C15S Cr-TRP16 show a single

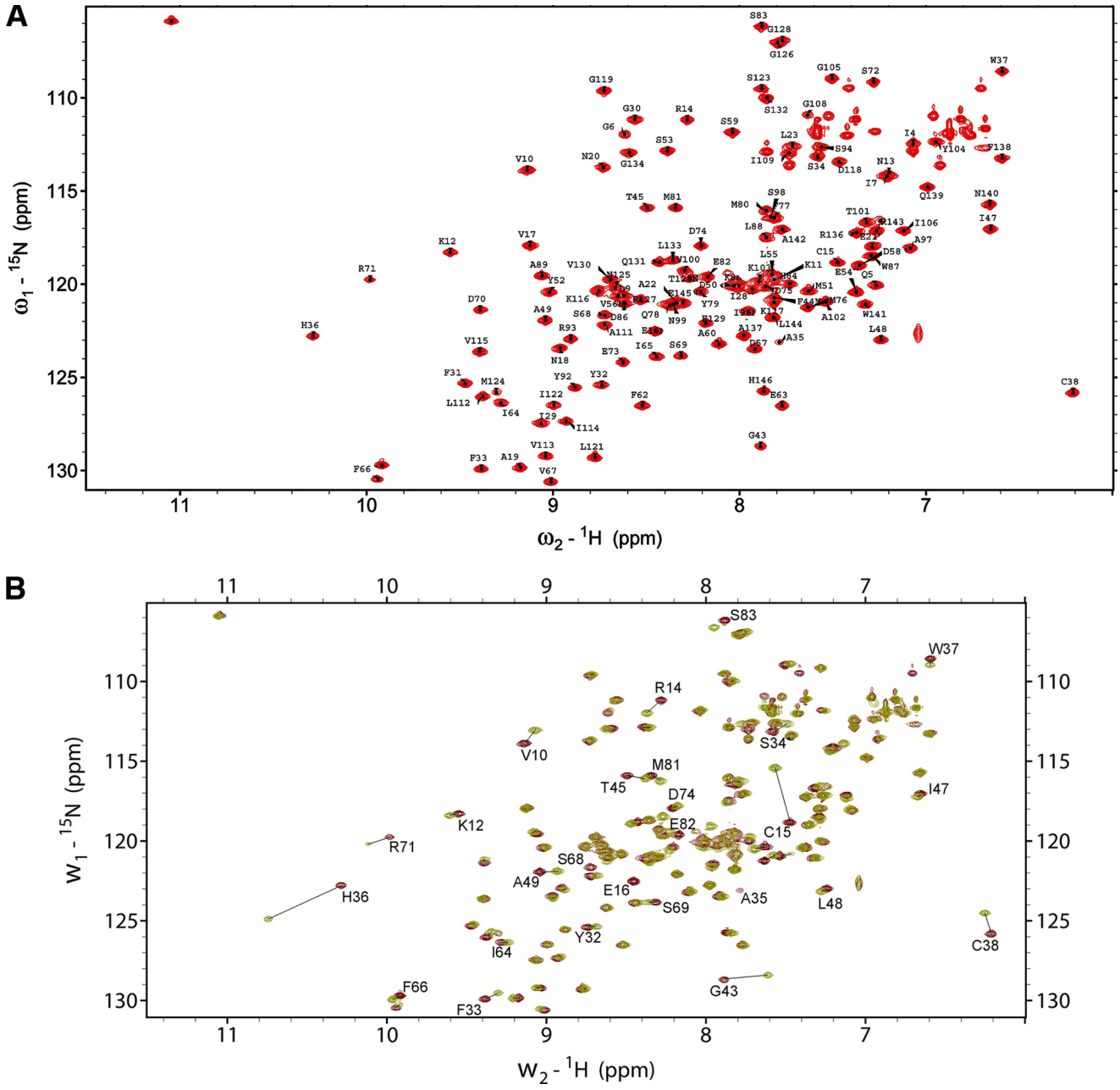

FIGURE 3. **Superposition of ^{1}H-^{15}N HSQC spectra of oxidized and reduced wild type Cr-TRP16 ^{1}H-^{15}N HSQC spectra of CrTRP16 in its reduced (*A*) and overlay of oxidized and reduced forms (*B*).** Backbone amide resonances are labeled according to sequential assignments. *Lines* indicate shifts displayed by amino acid residues participating in the interactions leading to dimerization. The spectra were acquired at 303 K in 10 mM Tris-HCl buffer (pH 7.0).

band at an apparent molecular mass of 17 kDa (Fig. 4*C*), whereas nonreducing PAGE for the wild type protein shows an apparent dimer band (at 34 kDa). In the AUC analysis of oxidized wild type Cr-TRP16 protein ($A_{280\,nm}$ = 0.8), there is only one peak corresponding to an apparent molecular mass of a dimeric Cr-TRP16 (34 kDa; Fig. 4*A*, *panel i*), whereas the reduced Cr-TRP16 protein shows a peak at 17 kDa, corresponding to monomeric Cr-TRP16 (Fig. 4*A*, *panel ii*). On the other hand, we observed only one peak with an apparent molecular mass of 17 kDa for both the oxidized (Fig. 4*B*, *panel i*) and reduced (Fig. 4*B*, *panel ii*) C15S mutant of Cr-TRP16. These results are in agreement with our hypothesis that Cys-15 is responsible for dimerization.

Cr-TRP16 Increases TNF-α-induced Nuclear Translocation of p65 and p50—Biophysical and mutational studies have confirmed that Cr-TRP16 exists as a dimer, and Cys-15 is responsible for its dimerization. However, it is unclear whether Cr-TRP16 exists as a dimer under physiological conditions. To address this, we expressed the wild type and C15S mutant Cr-TRP16 proteins and stimulated the cells with TNF-α, one of the most potent inducers of NF-κB activation (43). Western blot analysis with anti-p50 antibody revealed minimal change in the NF-κB p50 protein, suggesting that the overexpression of Cr-TRP16 does not change the expression of p50 (Fig. 5*A*). Similarly it does not show any significant effect on the TNF-α induced IκBα degradation (Fig. 5*C*). Subsequently, we investi-

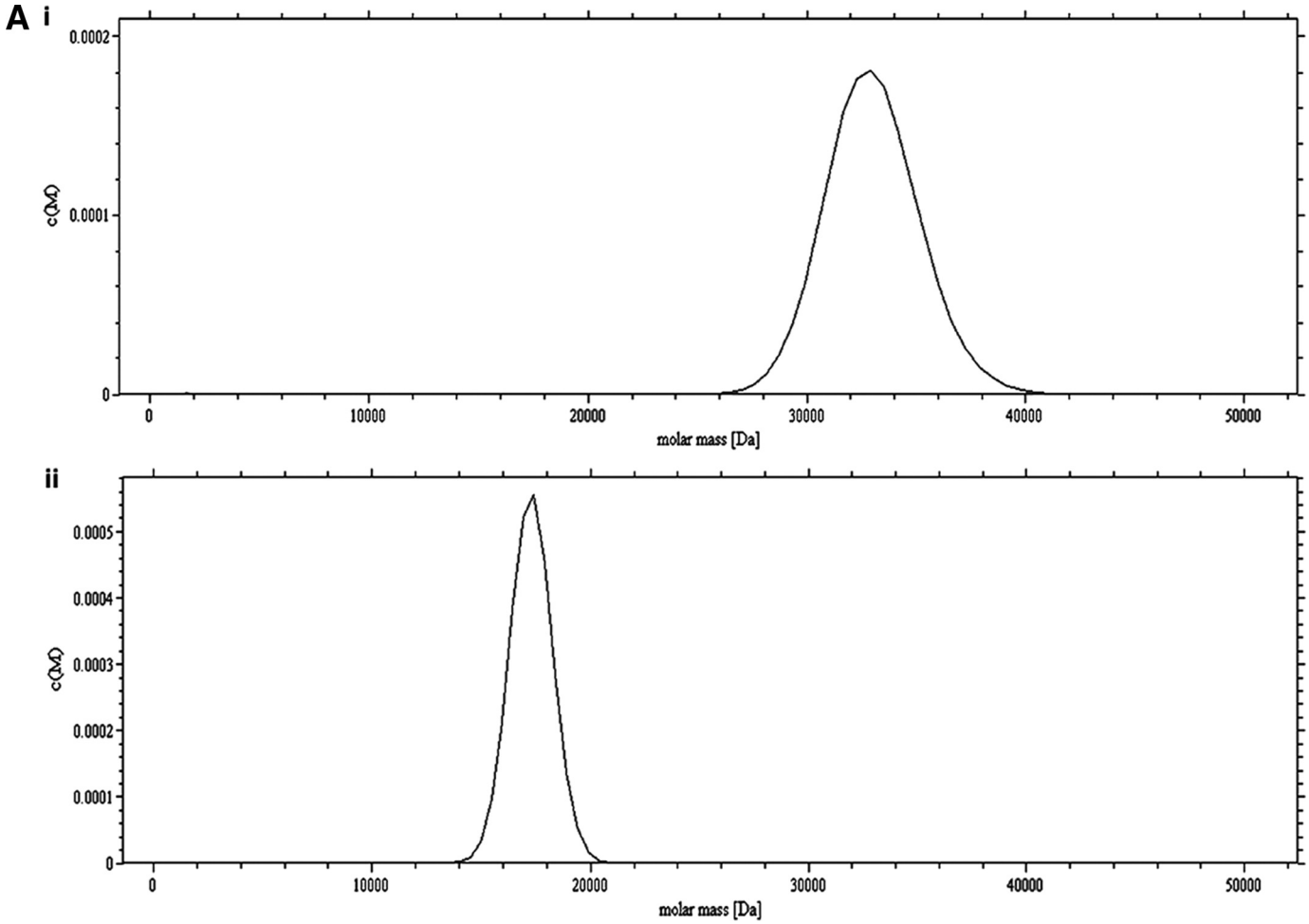

FIGURE 4. **Study of the dimerization of Cr-TRP16 by sedimentation velocity analysis.** The experiments were conducted in TRIS buffer (10 mM Tris-HCl (pH 7.0), 100 mM NaCl, and 5% glycerol) at a rotor speed of 40,000 rpm, and a rotor temperature of 20 °C. The experiments were carried out in the absence of DTT in the buffer. The sedimentation velocity profiles were collected by monitoring the absorbance at 280 nm. *A*, molecular mass profile of oxidized (*panel i*) and reduced (*panel ii*) wild type Cr-TRP16. *B*, molecular mass profile of oxidized (*panel i*) and reduced (*panel ii*) C15S Cr-TRP16. The scans were analyzed using Sedfit program (33). *C*, SDS-PAGE analysis of Cr-TRP16 dimerization. FPLC-purified Cr-TRP16 was subjected to reversed phase HPLC by using a C_8 column. The separated proteins were analyzed by SDS-PAGE and Coomassie Blue staining under nonreducing (−*DTT*) and reducing (+*DTT*) conditions, as indicated. *Lanes 2* and *3* represent oxidized and reduced wild type Cr-TRP16, respectively, under a nonreducing condition. Similarly *lanes 4* and *5* represent C15S mutant Cr-TRP16 under a nonreducing condition. *Lanes 5–8* represent similar loading patterns under a reducing (+*DTT*) SDS-PAGE condition as indicated earlier. A molecular marker is shown in *lane 1* of the gel. This analysis shows that only wild type Cr-TRP16 can form a dimer.

gated the effect of Cr-TRP16 overexpression on nuclear translocation of NF-κB. Western blot analysis with nuclear extract using anti-p50, anti-p65, and anti-phosphorylated p65 antibodies revealed that the overexpression of wild type Cr-TRP16 induced the nuclear translocation of the p50-p65 heterodimer and increased the level of phosphorylated p65, whereas no appreciable increase was observed in C15S Cr-TRP16-transfected cells (Fig. 5, *B* and *C*).

Cr-TRP16 Augments TNFα-induced NF-κB DNA Binding Activity—Next we investigated the effect of wild type and C15S mutant Cr-TRP16 on NF-κB DNA binding activity. Nuclear extracts were prepared and tested for NF-κB activity using an ELISA-based DNA binding assay. Fig. 6*A* demonstrates that wild type Cr-TRP16 increases TNF-α induced NF-κB DNA binding activity, whereas there is no significant change observed in the C15S Cr-TRP16-transfected cells. These results clearly indicate that overexpression of Cr-TRP16 significantly enhances TNF-α induced NF-κB activation in HeLa cells.

Cr-TRP16 Augments TNF-α-induced NF-κB-dependent Reporter Gene Expression—Although we observe that Cr-TRP16 increases NF-κB activation in the NF-κB DNA binding assay, DNA binding alone does not always correlate with NF-κB-dependent gene transcription, indicating there could be some additional regulatory steps (44). To determine the effects of Cr-TRP16 on TNF-α-induced NF-κB-dependent reporter gene expression, we transiently transfected HeLa cells with Cr-TRP16 or C15S Cr-TRP16 along with NF-κB to regulate a luciferase reporter construct and co-transfected with a β-galactosidase vector. A 2-fold increase in luciferase activity was observed after stimulation with TNF-α alone (Fig. 6*B*), whereas the wild type Cr-TRP16-transfected HeLa cells show a 6-fold increase in TNF-α-mediated NF-κB-dependent luciferase expression. Interestingly, no significant effect was observed in the cells transfected with C15S Cr-TRP16. These results show that Cr-TRP16 can potentiate TNF-α-inducible NF-κB-dependent reporter gene expression.

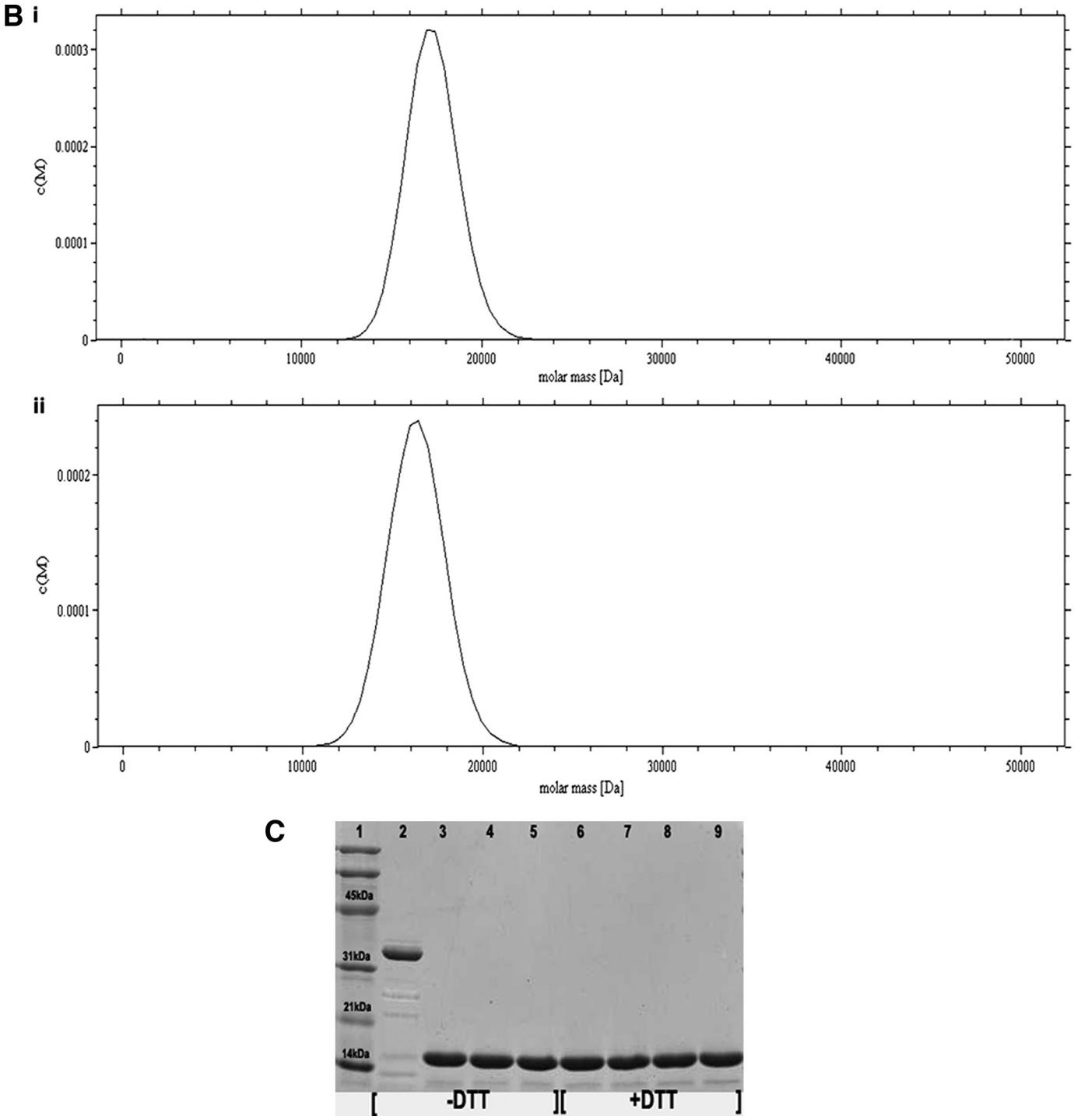

FIGURE 4 —*continued*

Effect of Cr-TRP16 on DNA Binding of NF-κB/p65 C38S Mutant—The mammalian NF-κB family includes five related proteins (p50, p52, p65, c-Rel, and RelB) that form various combinations of homo- and heterodimers to control the activity of numerous genes. Both p50 NF-κB and p65 NF-κB have redox-sensitive Cys residues that must be in the reduced state for the proteins to participate in transcriptional regulation. The binding of NF-κB to DNA requires that the Cys-62 of the NF-κB p50 subunit or Cys-38 of the NF-κB p65 subunit be reduced (43). Previous studies showed that the C38S mutant of p65 NF-κB shows severalfold higher DNA binding activity (43, 45–47).

Our biophysical studies (AUC, nonreducing SDS, and two-dimensional NMR experiments), mutation, and TNF-α induced NF-κB DNA binding activity confirm that only wild type Cr-TRP16 forms a dimer under an oxidized condition and not the C15S mutant. Furthermore our experiment on the effect of Cr-TRP16 on DNA binding of the NF-κB-p65 C38S mutant shows that Cr-TRP16 directly reduces Cys-38 of the p65 NF-κB subunit and exists as dimer inside cells.

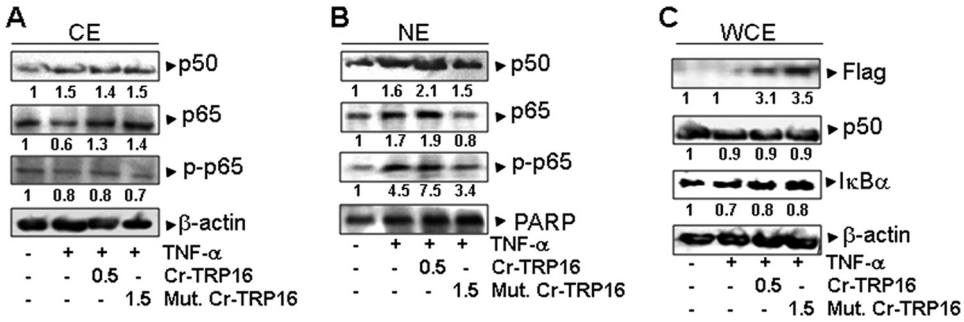

FIGURE 5. **Effect of Cr-TRP16 on the expression and subcellular localization of NF-κB.** *A*, effects of Cr-TRP16 expression on NF-κB p50, p65, and IκBα expression. HeLa cells were transfected with Cr-TRP16 as described under "Experimental Procedures." Whole cell lysates were subjected to Western blot analysis. The FLAG-tagged Cr-TRP16 was detected with anti-FLAG antibody. *B* and *C*, HeLa were transfected with the plasmids Cr-TR16 or C15S Cr-TRP16 for 30 h and then stimulated with TNF-α (1 nM) for 6 h. Nuclear and cytoplasmic protein extracts were prepared using nuclear extraction kit (Active Motif) according to the manufacturer's instructions. Protein concentration was determined with Bradford reagent. The nuclear and cytoplasmic extracts were subjected to Western blot analysis. The level of actin served as a loading control. *NE*, nuclear extract; *CE*, cytoplasmic extract; *WCE*, whole cell extract.

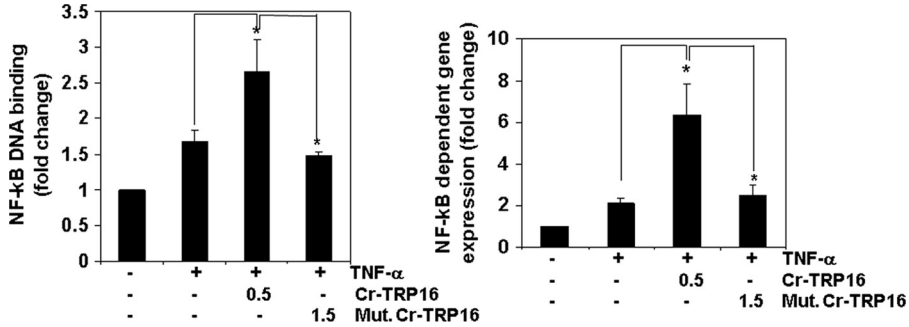

FIGURE 6. **Cr-TRP16 activates NF-κB in HeLa cells.** *A*, TNF-α induced NF-κB DNA binding activity. HeLa cells were transfected with indicated amounts of wild type and mutant (C15S) Cr-TRP16 for 30 h and then stimulated with TNF-α (1 nM) for 6 h. Nuclear extracts from HeLa cells stimulated with TNF-α were assayed for NF-κB p65 activation. Nuclear protein extracts were prepared using a nuclear extraction kit (Active Motif) according to the manufacturer's instructions and assayed for NF-κB p65 activation using the TransAM NFκB p65 kit. *B*, effect of overexpression of Cr-TRP16 on the NF-κB activity. HeLa cells were transfected with the indicated amounts of wild type and C15S Cr-TRP16 along with NF-κB regulate luciferase reporter construct and co-transfected with β-galactosidase vector. Luciferase activity was measured using luciferase assay kit (Promega). Relative light units were measured by a Tecan (Durham, NC) plate reader with the function of measuring luminescence, and the data were normalized to β-galactosidase activity. All of the luciferase experiments were done in triplicate and repeated three or more times.

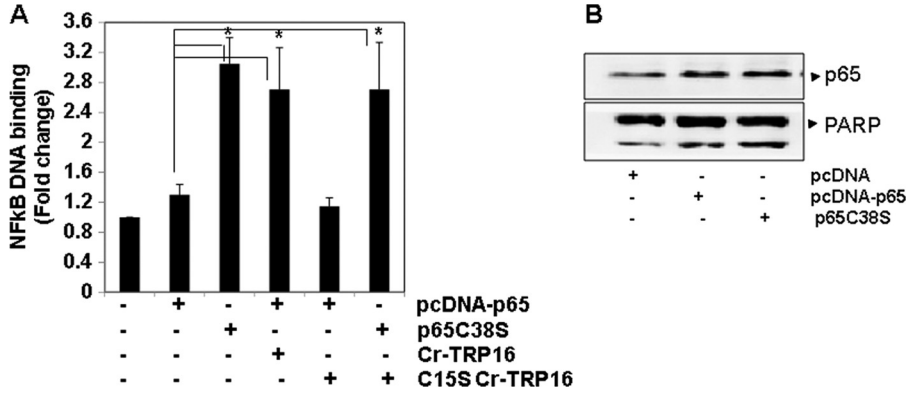

FIGURE 7. **Cr-TRP16 enhances NF-κB DNA binding activity by reducing cysteine residues on p65.** *A*, effect of wild type or C15S Cr-TRP16 on NF-κB activation. HeLa cells were transfected with 1 μg of pcDNA3.1 or pcDNA-p65 or pcDNA-p65C38S expression plasmid and co-transfected with indicated amounts of wild type and mutant Cr-TRP16 for 36 h, and then nuclear protein extracts were prepared using a nuclear extraction kit (Active Motif) according to the manufacturer's instructions. Nuclear extracts from HeLa cells were assayed for NF-κB p65 activation using the TransAM NF-κB p65 kit. *B*, HeLa cells were transfected with 1 μg of pcDNA3.1 or pcDNA-p65 or pcDNA-p65C38S expression plasmid. The nuclear extracts were subjected to Western blot analysis. The level of poly(ADP-ribose) polymerase served as loading control.

As shown in Fig. 7*A*, in the presence of Cr-TRP16 there is a 3-fold increase in the DNA binding activity of wild type p65. This experiment indicates that the enhancement of the DNA binding activity of wild type p65 is only due to reduction of Cys-38 of p65 by Cr-TRP16 (thereby increasing its DNA binding activity). However, C15S Cr-TRP16 could not enhance the wild type p65 activity. Overall, our results clearly demonstrate that the Cys-15 residue is crucial for the dimerization of Cr-TRP16, and only the dimeric form plays a pivotal role under physiological conditions in the regulation of NF-κB activation.

DISCUSSION

Sequence alignment reveals that the catalytic WCPPC motif is evolutionarily conserved and indicates the potential

importance of this motif even in 16-kDa Trx-like proteins. Although the active site of the 16-kDa Trx-like proteins in mammals has undergone marked changes, several other regions remain well conserved, when compared with the 12-kDa Trxs. This observation suggests that the members of the 16-kDa Trx-like protein family have evolutionarily diverged from the 12-kDa Trxs at an early stage, from *Caenorhabditis elegans* to human (17). Several multi-domain Trx-like proteins have evolved, retaining the Trx fold (49). Although the Trx superfamily has received much attention, only a few structural and functional studies have been undertaken to analyze the multi-domain Trx proteins. Cr-TRP16 has a fold similar to that of tryparedoxin, a 16-kDa Trx-like protein from the parasitic protozoa *C. fasciculate* (*Trypanosoma*) (50). In particular, the active site motif, CPPC, is homologous to that of the corresponding motif in the protozoan Trx-like protein (51). However, functionally the Cr-TRP16 is quite different from the tryparedoxin. In contrast, despite notable differences in the amino acid sequence of the catalytic site, Cr-TRP16 appears to be functionally similar to human Trx (52) and regulates NF-κB activity (17).

Although most of the 16-kDa Trx-like proteins do not have an extra cysteine, Cr-TRP16 possesses an additional Cys residue at the N terminus. Therefore, it is important to identify which Cys residue is redox-sensitive in Cr-TRP16. Our previous studies have shown that only Cys-38 and Cys-41 are redox-sensitive (17). However, Cys-15 could not react with iodoacetamide and remains inactive toward redox reactions. This prompted us to investigate the functional significance of this Cys and hypothesize that Cr-TRP16 could form a homodimer and regulate NF-κB, like hTrx1. Mutation, AUC, nonreducing SDS, and two-dimensional NMR experiments all confirm that only wild type Cr-TRP16 can form a dimer under an oxidized condition and not the C15S mutant. However, it was unclear whether the dimer or monomer is the active form *in vivo*.

To clarify the physiological role of the N-terminal Cys-15 residue of Cr-TRP16, we overexpressed the wild type and C15S mutant proteins in HeLa cells, stimulated the cells with TNF-α, and measured NF-κB activation. We found that wild type Cr-TRP16 could increase the TNF-α induced NF-κB DNA binding activity but not the C15S mutant-transfected cells (Fig. 6). Moreover, we observed a similar pattern of results in TNF-α-induced NF-κB-dependent luciferase expression in the cells that were transfected with wild type and C15S mutant (Fig. 7).

The Cys-38 residue in the p65 subunits of NF-κB has been identified to be crucial for DNA binding (47). We investigated the molecular mechanism by which Cr-TRP16 directly reduces Cys-38 of the NF-κB p65 subunit and exists as dimer inside the cell. We found that in the presence of wild type Cr-TRP16, there is a 3-fold increase in the DNA binding activity of wild type p65 (Fig. 7*A*). However, C15S could not enhance the p65 activity. Thus, our results suggest that the dimeric form of Cr-TRP16 must modify this cysteine residue of p65, leading to NF-κB DNA binding activity.

Even though the C15S mutant contains intact redox-active Cys-38 and Cys-41 residues, it could not regulate the NF-κB activity, suggesting that Cr-TRP16 exists as a dimer under the

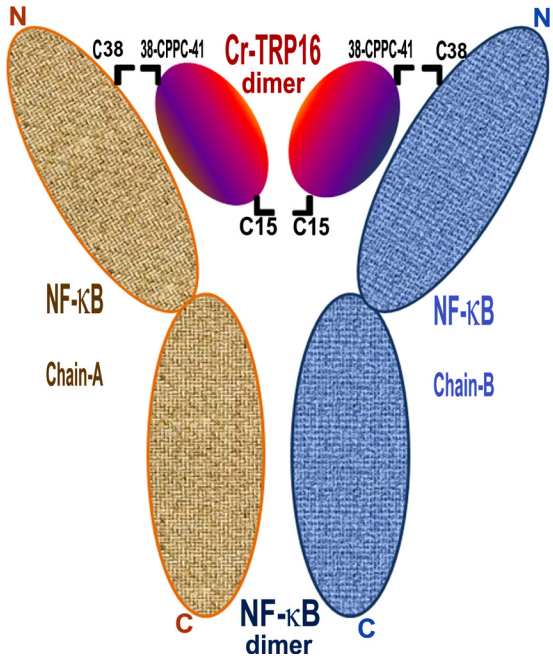

FIGURE 8. **Model for the interaction of Cr-TRP16 dimer with NF-κB dimer.** Based on the previously published human NF-κB p50 homodimer-DNA complex and human Trx-NF-κB p50 peptide complex structures and our structural, biophysical, and biochemical results, we propose that Cr-TRP16 forms a homodimer by making a disulfide link through Cys-15 and is likely to occupy the location where DNA binds to NF-κB. The active site motif WCPPC of Cr-TRP16 (through Cys-38 and Cys-41) is likely to interact with the redox active Cys-62 of NF-κB dimer. For the ease of residue numbering, a p50 homodimer is assumed for NF-κB, and the C-terminal cysteines of NF-κB that promote dimerization of NF-κB are not shown for simplicity.

physiological condition and that Cys-15 is the crucial residue for the dimer formation. Similar to human Trx1, Cr-TRP16 also up-regulates TNFα-induced NF-κB activation. Interestingly, although Cr-TRP16 lacks the C-terminal extra Cys residue, it forms a dimer with a molecular mass of 32 kDa via N-terminal Cys-15. In addition, human Trx1 is a protein highly homologous to Cr-TRP16 and shares 54% sequence similarity. Notably, it has been reported that the NF-κB-modulating activity is rather conserved in human TXN-6 (a thioredoxin like protein-6) because it could cross-enhance the horseshoe crab NF-κB DNA binding activity as well (34), suggesting the functional conservation among the 16-kDa Cr-TRP16 and 24-kDa human Trxs. Therefore, it is reasonable to postulate that similar to the human Trx1 dimer (23, 53), dimeric Cr-TRP16 reduces Cys-38 in the human p65 N-κB DNA-binding motif to enhance its DNA binding activity. These results are consistent with our biophysical studies and the present evidence that the dimer of Cr-TRP16 is the naturally occurring form.

Studies by Matthews *et al.* (23) and Meyer *et al.* (54) show that the DNA binding activity of NF-κB follows redox regulation through its modulatory Cys residues. Furthermore, the NF-κB subunits, p50 and p65, contain well conserved cysteine residues in their DNA-binding loops (55, 56). Activation of the DNA binding properties of human NF-κB requires that the Cys-62 of the p50 subunit and Cys-38 of p65 subunit be reduced. In the p50 homodimer-DNA complex structure (55, 56), the p65 homodimer binds to DNA in a channel, wherein one end is closed by the C-terminal dimerization domain, and

the front is closed by two loops that contain Cys-38, one from each subunit. If a disulfide is formed between the two Cys-38 residues in uncomplexed NF-κB, then DNA cannot bind to the p65 homodimer. Similarly, if a disulfide bridge is formed in the p65 homodimer-DNA complex, then DNA cannot be released (52). This implies that the activation of NF-κB DNA binding activity begins with IκB degradation, reduction of NF-κB by Trx followed by translocation of NF-κB to the nucleus (57, 58) for effective DNA binding and transactivation (58). Based on this argument and our structure-function analyses, we propose a model on how Cr-TRP16 could bind to the p65 homodimer or p50/p65 heterodimer *in vivo* (Fig. 8).

Several diseases, including cancer, autoimmune diseases, and infectious diseases, are mediated through the effects of Trx and Trx reductase and imbalance in NF-κB activation. The structure-based functional studies clearly demonstrated that 1) Cr-TRP16 regulates NF-κB similar to the 12 kDa human Trx, 2) Cys-15 is the key residue for dimerization, and 3) only the dimeric Cr-TRP16 regulates NF-κB activity. This study helps in further understanding of the interactions of Trxs and Trx-like proteins with other metabolic pathways and their physiological relevance, which will lead to promising therapeutic development to modulate the actions of Trx and NF-κB.

REFERENCES

1. Valko, M., Leibfritz, D., Moncol, J., Cronin, M. T., Mazur, M., and Telser, J. (2007) Free radicals and antioxidants in normal physiological functions and human disease. *Int. J. Biochem. Cell Biol.* **39,** 44–84
2. Marnett, L. J. (2000) Oxyradicals and DNA damage. *Carcinogenesis* **21,** 361–370
3. Nordberg, J., and Arnér, E. S. (2001) Reactive oxygen species, antioxidants, and the mammalian thioredoxin system. *Free Radic. Biol. Med.* **31,** 1287–1312
4. Holmgren, A. (1995) Thioredoxin structure and mechanism. Conformational changes on oxidation of the active-site sulfhydryls to a disulfide. *Structure* **3,** 239–243
5. Arnér, E. S., and Holmgren, A. (2000) Physiological functions of thioredoxin and thioredoxin reductase. *Eur. J. Biochem.* **267,** 6102–6109
6. Powis, G., and Montfort, W. R. (2001) Properties and biological activities of thioredoxins. *Annu. Rev. Biophys. Biomol. Struct.* **30,** 421–455
7. Carvalho, A. P., Fernandes, P. A., and Ramos, M. J. (2006) Similarities and differences in the thioredoxin superfamily. *Prog. Biophys. Mol. Biol.* **91,** 229–248
8. Liu, H., Nishitoh, H., Ichijo, H., and Kyriakis, J. M. (2000) Activation of apoptosis signal-regulating kinase 1 (ASK1) by tumor necrosis factor receptor-associated factor 2 requires prior dissociation of the ASK1 inhibitor thioredoxin. *Mol. Cell. Biol.* **20,** 2198–2208
9. Aviram, M. (2000) Review of human studies on oxidative damage and antioxidant protection related to cardiovascular diseases. *Free Radic. Res.* **33,** S85-S97
10. Davì, G., Falco, A., and Patrono, C. (2005) Lipid peroxidation in diabetes mellitus. *Antioxid. Redox Signal.* **7,** 256–268
11. Seki, S., Kitada, T., Yamada, T., Sakaguchi, H., Nakatani, K., and Wakasa, K. (2002) *In situ* detection of lipid peroxidation and oxidative DNA damage in non-alcoholic fatty liver diseases. *J. Hepatol.* **37,** 56–62
12. Nunomura, A., Castellani, R. J., Zhu, X., Moreira, P. I., Perry, G., and Smith, M. A. (2006) Involvement of oxidative stress in Alzheimer disease. *J. Neuropathol. Exp. Neurol.* **65,** 631–641
13. Wood-Kaczmar, A., Gandhi, S., and Wood, N. W. (2006) Understanding the molecular causes of Parkinson's disease. *Trends Mol. Med.* **12,** 521–528
14. Hitchon, C. A., and El-Gabalawy, H. S. (2004) Oxidation in rheumatoid arthritis. *Arthritis Res. Ther.* **6,** 265–278
15. Fujii, S., Nanbu, Y., Nonogaki, H., Konishi, I., Mori, T., Masutani, H., and Yodoi, J. (1991) Coexpression of adult T-cell leukemia-derived factor, a human thioredoxin homologue, and human papillomavirus DNA in neoplastic cervical squamous epithelium. *Cancer* **68,** 1583–1591
16. Gasdaska, P. Y., Oblong, J. E., Cotgreave, I. A., and Powis, G. (1994) The predicted amino acid sequence of human thioredoxin is identical to that of the autocrine growth factor human adult T-cell derived factor (ADF). Thioredoxin mRNA is elevated in some human tumors. *Biochim. Biophys. Acta* **1218,** 292–296
17. Wang, X. W., Liou, Y. C., Ho, B., and Ding, J. L. (2007) An evolutionarily conserved 16-kDa thioredoxin-related protein is an antioxidant which regulates the NF-κB signaling pathway. *Free Radic. Biol. Med.* **42,** 247–259
18. Weichsel, A., Gasdaska, J. R., Powis, G., and Montfort, W. R. (1996) Crystal structures of reduced, oxidized, and mutated human thioredoxins. Evidence for a regulatory homodimer. *Structure* **4,** 735–751
19. Sen, C. K., and Packer, L. (1996) Antioxidant and redox regulation of gene transcription. *FASEB J.* **10,** 709–720
20. Verma, I. M. (2004) Nuclear factor (NF)-κB proteins. Therapeutic targets. *Ann. Rheum. Dis.* **63,** ii57–ii61
21. Menon, S. D., Guy, G. R., and Tan, Y. H. (1995) Involvement of a putative protein-tyrosine phosphatase and IκB-α serine phosphorylation in nuclear factor κB activation by tumor necrosis factor. *J. Biol. Chem.* **270,** 18881–18887
22. Zabel, U., and Baeuerle, P. A. (1990) Purified human IκB can rapidly dissociate the complex of the NF-κB transcription factor with its cognate DNA. *Cell* **61,** 255–265
23. Matthews, J. R., Wakasugi, N., Virelizier, J. L., Yodoi, J., and Hay, R. T. (1992) Thioredoxin regulates the DNA binding activity of NF-κB by reduction of a disulphide bond involving cysteine 62. *Nucleic Acids Res.* **20,** 3821–3830
24. Ren, X., Björnstedt, M., Shen, B., Ericson, M. L., and Holmgren, A. (1993) Mutagenesis of structural half-cystine residues in human thioredoxin and effects on the regulation of activity by selenodiglutathione. *Biochemistry* **32,** 9701–9708
25. Bax, A., and Grzesiek, S. (1993) Methodological advances in protein NMR. *Acc. Chem. Res.* **26,** 131–138
26. Fesik, S. W., Eaton, H. L., Olejniczak, E. T., Zuiderweg, E. R., McIntosh, L. P., and Dahlquist, F. W. (1990) 2D and 3D NMR spectroscopy employing ^{13}C-^{13}C magnetization transfer by isotropic mixing. Spins system identification in large proteins. *J. Am. Chem. Soc.* **112,** 886–888
27. Ottiger, M., Delaglio, F., and Bax, A. (1998) Measurement of J and dipolar couplings from simplified two-dimensional NMR spectra. *J. Magn. Reson.* **131,** 373–378
28. Delaglio, F., Grzesiek, S., Vuister, G. W., Zhu, G., Pfeifer, J., and Bax, A. (1995) NMRPipe. A multidimensional spectral processing system based on UNIX pipes. *J. Biomol. NMR* **6,** 277–293
29. Goddard, T. D., and Kneller, D. G. SPARKY 3, University of California, San Francisco
30. Schwieters, C. D., Kuszewski, J. J., Tjandra, N., and Clore, G. M. (2003) The Xplor-NIH NMR molecular structure determination package. *J. Magn. Reson.* **160,** 65–73
31. Cornilescu, G., Delaglio, F., and Bax, A. (1999) Protein backbone angle restraints from searching a database for chemical shift and sequence homology. *J. Biomol. NMR* **13,** 289–302
32. Ochman, H., Gerber, A. S., and Hartl, D. L. (1988) Genetic applications of an inverse polymerase chain reaction. *Genetics* **120,** 621–623
33. Brown, P. H., and Schuck, P. (2006) Macromolecular size-and-shape distributions by sedimentation velocity analytical ultracentrifugation. *Biophys. J.* **90,** 4651–4661
34. Wang, X. W., Tan, B. Z., Sun, M., Ho, B., and Ding, J. L. (2008) Thioredoxin-like 6 protects retinal cell line from photooxidative damage by up-regulating NF-κB activity. *Free Radic. Biol. Med.* **45,** 336–344
35. Urban, M. B., Schreck, R., and Baeuerle, P. A. (1991) NF-κB contacts DNA by a heterodimer of the p50 and p65 subunit. *EMBO J.* **10,** 1817–1825
36. Renard, P., Ernest, I., Houbion, A., Art, M., Le Calvez, H., Raes, M., and Remacle, J. (2001) Development of a sensitive multi-well colorimetric assay for active NFκB. *Nucleic Acids Res.* **29,** E21
37. Mukhopadhyay, A., Bueso-Ramos, C., Chatterjee, D., Pantazis, P., and Aggarwal, B. B. (2001) Curcumin downregulates cell survival mechanisms

in human prostate cancer cell lines. *Oncogene* **20,** 7597–7609
38. Matsuo, Y., Hirota, K., Nakamura, H., and Yodoi, J. (2002) Redox regulation by thioredoxin and its related molecules. *Drug News Perspect.* **15,** 575–580
39. Eklund, H., Gleason, F. K., and Holmgren, A. (1991) Structural and functional relations among thioredoxins of different species. *Proteins Struct. Funct. Genet.* **11,** 13–28
40. Holm, L., and Sander, C. (1998) Touring protein fold space with Dali/FSSP. *Nucleic Acids Res.* **26,** 316–319
41. Martin, J. L. (1995) Thioredoxin. A fold for all reasons. *Structure* **3,** 245–250
42. Laskowski, R. A., Rullmannn, J. A., MacArthur, M. W., Kaptein, R., and Thornton, J. M. (1996) AQUA and PROCHECK-NMR. Programs for checking the quality of protein structures solved by NMR. *J. Biomol. NMR* **8,** 477–486
43. Sethi, G., and Tergaonkar, V. (2009) Potential pharmacological control of the NF-κB pathway. *Trends Pharmacol. Sci.* **30,** 313–321
44. Ahn, K. S., Sethi, G., and Aggarwal, B. B. (2007) Nuclear factor-κB. From clone to clinic. *Curr. Mol. Med.* **7,** 619–637
45. Liang, M. C., Bardhan, S., Pace, E. A., Rosman, D., Beutler, J. A., Porco, J. A., Jr., and Gilmore, T. D. (2006) Inhibition of transcription factor NF-κB signaling proteins IKKβ and p65 through specific cysteine residues by epoxyquinone A monomer. Correlation with its anti-cancer cell growth activity. *Biochem. Pharmacol.* **71,** 634–645
46. Sethi, G., Ahn, K. S., and Aggarwal, B. B. (2008) Targeting nuclear factor-κB activation pathway by thymoquinone. Role in suppression of antiapoptotic gene products and enhancement of apoptosis. *Mol. Cancer Res.* **6,** 1059–1070
47. García-Piñeres, A. J., Castro, V., Mora, G., Schmidt, T. J., Strunck, E., Pahl, H. L., and Merfort, I. (2001) Cysteine 38 in p65/NF-κB plays a crucial role in DNA binding inhibition by sesquiterpene lactones. *J. Biol. Chem.* **276,** 39713–39720
48. Koradi, R., Billeter, M., and Wüthrich, K. (1996) MOLMOL. A program for display and analysis of macromolecular structures. *J. Mol. Graphics* **14,** 51–55
49. Atkinson, H. J., and Babbitt, P. C. (2009) An atlas of the thioredoxin fold class reveals the complexity of function-enabling adaptations. *PLoS Comput. Biol.* **5,** e1000541
50. Montemartini, M., Steinert, P., Singh, M., Flohé, L., and Kalisz, H. M. (2000) Tryparedoxin II from *Crithidia fasciculata*. *Biofactors* **11,** 65–66
51. Hofmann, B., Budde, H., Bruns, K., Guerrero, S. A., Kalisz, H. M., Menge, U., Montemartini, M., Nogoceke, E., Steinert, P., Wissing, J. B., Flohé, L., and Hecht, H. J. (2001) Structures of tryparedoxins revealing interaction with trypanothione. *Biol. Chem.* **382,** 459–471
52. Qin, J., Clore, G. M., Kennedy, W. M., Huth, J. R., and Gronenborn, A. M. (1995) Solution structure of human thioredoxin in a mixed disulfide intermediate complex with its target peptide from the transcription factor NF κB. *Structure* **3,** 289–297
53. Hirota, K., Nakamura, H., Masutani, H., and Yodoi, J. (2002) Thioredoxin superfamily and thioredoxin-inducing agents. *Ann. N.Y. Acad. Sci.* **957,** 189–199
54. Meyer, M., Schreck, R., and Baeuerle, P. A. (1993) H_2O_2 and antioxidants have opposite effects on activation of NF-κB and AP-1 in intact cells. AP-1 as secondary antioxidant-responsive factor. *EMBO J.* **12,** 2005–2015
55. Ghosh, G., van Duyne, G., Ghosh, S., and Sigler, P. B. (1995) Structure of NF-κB p50 homodimer bound to a κB site. *Nature* **373,** 303–310
56. Müller, C. W., Rey, F. A., Sodeoka, M., Verdine, G. L., and Harrison, S. C. (1995) Structure of the NF-κB p50 homodimer bound to DNA. *Nature* **373,** 311–317
57. Powis, G., and Montfort, W. R. (2001) Properties and biological activities of thioredoxins. *Annu. Rev. Pharmacol. Toxicol.* **41,** 261–295
58. Flohé, L., Brigelius-Flohé, R., Saliou, C., Traber, M. G., and Packer, L. (1997) Redox regulation of NF-κB activation. *Free Radic. Biol. Med.* **22,** 1115–1126
59. Kraulis, P. (1991) Molscript. A program to produce both detailed and schematic plots of protein structures. *J. Appl. Crystallogr.* **24,** 946–950
60. Gouet, P., Courcelle, E., Stuart, D. I., and Métoz, F. (1999) ESPript. Analysis of multiple sequence alignments in PostScript. *Bioinformatics* **15,** 305–308
61. Emsley, P., and Cowtan, K. (2004) Coot. Model-building tools for molecular graphics. *Acta Crystallogr. D Biol. Crystallogr.* **60,** 2126–2132